University of Sistan and Baluchestan

Challenges in Nano and Micro Scale Science and Technology

Online ISSN: 2821 - 000X

Tailoring of Band Gap Value of Metal Oxides - Graphene Oxide Nano Composites

Mahdi Shafiee Afarani✉ | **Salman Mahaki** | **Hamed Khosravi**

Department of Materials Engineering, Faculty of Engineering, University of Sistan and Baluchestan, Zahedan, Iran.
Corresponding Author's Email: shafiee@eng.usb.ac.ir

Article Info

Article type:
Research Article

Article history:
Received: 18 April 2026
Received in revised form: 16 May 2026
Accepted: 20 May 2026
Published Online: 20 May 2026

Keywords:
Nanocomposite,
Graphene oxide nanoplatelets,
Metal oxide,
Precipitation,
Band gap

ABSTRACT

Copper oxide (CuO), zinc oxide (ZnO), iron oxide (Fe_2O_3) and manganese oxide (Mn_3O_4) nano particles were in-situ synthesized on the graphene oxide (GO) nano platelets via precipitation method using hydrated metal salts and NaOH starting materials. The effect of composite formation on the structure, microstructure and band gap of nano composite samples were investigated. Results generally showed that crystalline phase of metal oxides was formed on the graphene oxide (GO) nanoplatelets. Furthermore, Fourier transform infrared (FTIR) spectra illustrated the corresponding bands of metal–oxygen bonds in all samples. In addition, Field emission scanning electron micrographs (FE- SEM) showed that nanoparticles were synthesized on the surface of graphene oxide nanoplatelets which were agglomerated in some areas. Moreover, Uv-Vis spectra of all nano composite samples were plotted. Composites represented lower optical band gap values than those of pure graphene oxide nanoplatelets due to formation of Interfacial charge transfer and Schottky junctions.

INTRODUCTION

The synthesis of metal oxide - graphene oxide nano composite particles has been extensively studied over the past two decades due to their interesting structural and functional properties, leading to a broad range of applications. For example, theses composites are highly attractive for the automotive industry because they can improve wear resistance, corrosion protection, mechanical strength, and thermal stability. These properties are important for extending the service life of automotive parts exposed to friction, harsh environments, and high temperatures. In addition, their lightweight nature can help reduce the overall weight of vehicle components, contributing to better fuel efficiency and lower emissions [1–3]. Other applications include energy storage devices [4], catalyst/photocatalysts [5–8], antibacterial and biomedical applications [9, 10] and graphene-based membranes [11].

Formation of metal oxide / graphene oxide (MO-GO) nanocomposites results in enhancing photocatalytic activity, adsorption capacity, charge carrier separation, and mechanical robustness [8, 11, 12]. Metal oxide nanoparticles were synthesized on graphene oxide nanoplatelets via several methods such as hydrothermal [9], precipitation [1–3], pulsed electrodeposition [13].

Some researchers showed that band gap values of MO-GO) nanocomposites were less than those of GO platelets. Different mechanisms were suggested for this phenomenon:

1-Interfacial charge transfer and Schottky junction formation:

A Schottky junction, also known as a rectifying metal–semiconductor contact, is formed when a metal is brought into intimate contact with a moderately or lightly doped semiconductor, leading to the establishment of a potential energy barrier at the interface [14, 15] MO nanoparticles anchored on GO sheets create a Schottky heterojunction, where the work function mismatch facilitates electron transfer from GO's conduction band to the MO Fermi level [16–18]. This depletes electrons from GO, shifting its Fermi level downward and narrowing the band gap [17]. For instance, in Fe_3O_4/GO composites, UV-Vis spectroscopy reveals a band gap drop from ~3.3 eV (pure GO) to 2.6 eV, attributed to new electronic states introduced by Fe-O-C bonds at the interface [16].

2- Partial reduction of GO and π-conjugation restoration: During composite synthesis (e.g., hydrothermal treatment), metal precursors or MO formation induces deoxygenation of GO, converting sp^3-hybridized carbons back to sp^2, which repairs π-conjugation and introduces mid-gap states [12, 17]. Raman

How to Cite this paper: Shafiee Afarani M. Mahaki S. Khosravi H. Tailoring of Band Gap Value of Metal Oxides - Graphene Oxide Nano Composites. *Challenges in Nano and Micro Scale Science and Technology*. 2026; 14(2): 31-36. DOI: 10.22111/cnmst.2026.55100.1294

DOI: 10.22111/cnmst.2026.55100.1294

spectroscopy confirms this via decreased I_D/I_G ratios (e.g., from 1.05 in GO to 0.92 in NiO/rGO), indicating defect healing and extended delocalization [18].

3- Chemical Doping and Defect State Introduction: Metal ions (e.g., Fe^{3+}, Ni^{2+}) dope into GO's lattice via oxygen bridges, creating impurity levels within the band gap that act as recombination centers or trap states, effectively narrowing the gap [16, 17]. XPS analysis shows increased C=C bonds and metal-oxygen coordination, supporting n-type doping that elevates the VBM [17].

Although lots of studies were performed on the in-situ synthesis of some metal oxides on the GO nanoplatelets such as CuO and ZnO, whereas researches on Fe_2O_3 and Mn_3O_4 are relatively scarce. Furthermore, various GO nanoplatelets are available in the world with different size and characteristics (i.e. band gap values). In this regards, copper, zinc, iron and manganese oxide nano particles were in-situ synthesized on the GO nanoplatelets via precipitation method. The effect of composite composition on the structure, microstructure and band gap of samples were investigated and compared.

Experimental

Copper chloride hexahydrate [$CuCl_2.6H_2O$, MERCK], Zinc chloride hexahydrate [$ZnCl_2.6H_2O$, MERCK], Iron chloride hexahydrate [$FeCl_2.6H_2O$, MERCK], Manganese nitrate nonahydrate [$Mn(NO_3)_2.9H_2O$, MERCK], Sodium hydroxide (NaOH, MERCK) and Graphene oxide nanoplatelets (GO, 10–50 µm in diameter, 3.4–7 nm in thickness, 6–10 layers, purity>99%, US Research Nanomaterials Inc) were used as starting materials. XRD pattern and SEM micrograph of the as received GONPs are shown in Figure 1a &b, respectively. As illustrated, a specific peak in 2θ = 11° can be observed, which relates to the (001) basal plane [1]. The synthesis of metal oxide particles on GO nano platelets was performed based on the work of Mohseni et.al [3]. First, 0.3 g of GO were dispersed in 140 ml of distilled water in a volumetric flask using magnetic stirrer for 1 hour at room temperature. Then, 10 ml of an aqueous (5 M) metal salt solutions was drop-wise added to the suspension of GONPs and mixed under magnetic stirring at 90 °C for 4 hours. Thereafter, 10 ml of NaOH (3 M) was drop-wise added into the suspensions and agitated at 90 °C for 10 min to precipitate metal oxides on the surface of GO nano platelets. Finally, the obtained samples were washed and dried at 80°C for 1h in an electric oven.

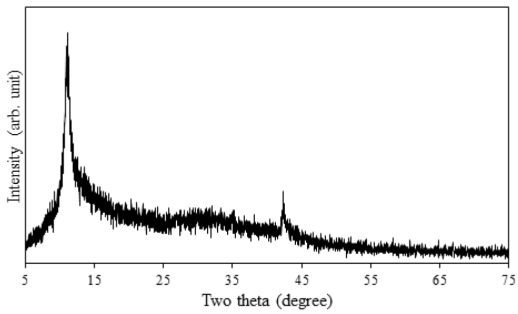

(a)

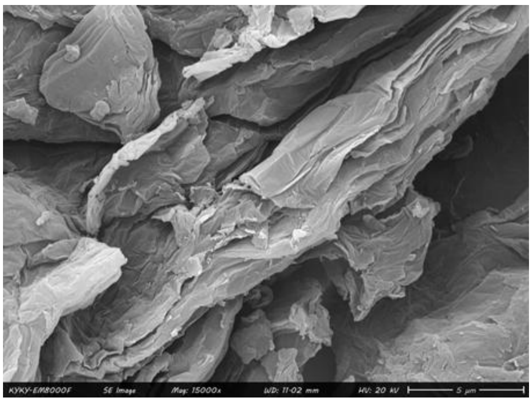

(b)

Fig. 1. a) XRD pattern and b) SEM micrograph of the GO platelets

All sample characterizations were performed at room temperature. A Fourier transform infrared spectroscope (FTIR, Bruker TENSOR II) which was equipped with platinum ATR accessory with the robust diamond crystal was used for molecular studies. Structural and microstructure characterizations of samples were performed using X-ray diffraction technique (XRD, Philips PW1730) with CuKα varing 2θ= 10 to 80° and field emission scanning electron microscopy (FESEM, KYKY EM8000F) equipped with EDS detector, respectively. UV-visible absorption spectra were drawn using a UV–Vis spectrophotometer (Agilent, Carry 60). Band gaps of samples were estimated by plotting $(\alpha h\nu)^2$ versus hν, based on the Tauc equation according to [19, 20], where α is absorption coefficient, h is Plank constant and ν is frequency (s^{-1}).

RESULTS AND DISCUSSIONS

X-ray diffraction (XRD) patterns of GO/MO samples are illustrated in figure 2a-d. As shown, all samples exhibit highest peak of Graphene oxide (Card No. 01-080-1268) at about 2Θ=12.7 degree. Moreover, monoclinic morenite CuO (Card No. 00-041-0254), hexagonal zinc oxide (01-079-2205), Hausmannite Mn_3O_4 (Card No. 01-024-0734) and maghemite Fe_2O_3 (00-025-1402) were formed as secondary phases correspondingly.

Figure 3 shows the FTIR spectra of the samples. In GO spectrum a broad band in the region of 3655-2400 cm^{-1} is associated to acidic O−H bond. Moreover, the bands at 1711, 1613 and 1044 are attributed to C=O, C=C and C−O bonds, respectively. In the GO/CuO spectrum, the main band at about 409 cm^{-1} is attributed to bending Cu-O bonds. Also, the bands at about 529 and 602 cm^{-1} are associated with stretching Cu-O bonds [21]. In the GO/Mn_3O_4 spectrum, the main band at about 405 cm^{-1} belongs to bending Mn-O bonds. Also, the bands at about 510 & 613 cm^{-1} are due to stretching Mn-O bonds [22]. In the GO/Fe_2O_3 spectrum, the main band at about 429 cm^{-1} is attributed to Fe−O bonds. Also, the bands at about 626 & 693 cm^{-1} belong to stretching Fe−O bonds [2, 23]. In the GO/ZnO spectrum, the main band at about 451 cm^{-1} is attributed to Zn−O bonds [24, 25]. The significant decrease in transmittance peak and the reduced oxygen-containing functional groups from GO to GO/MO explain

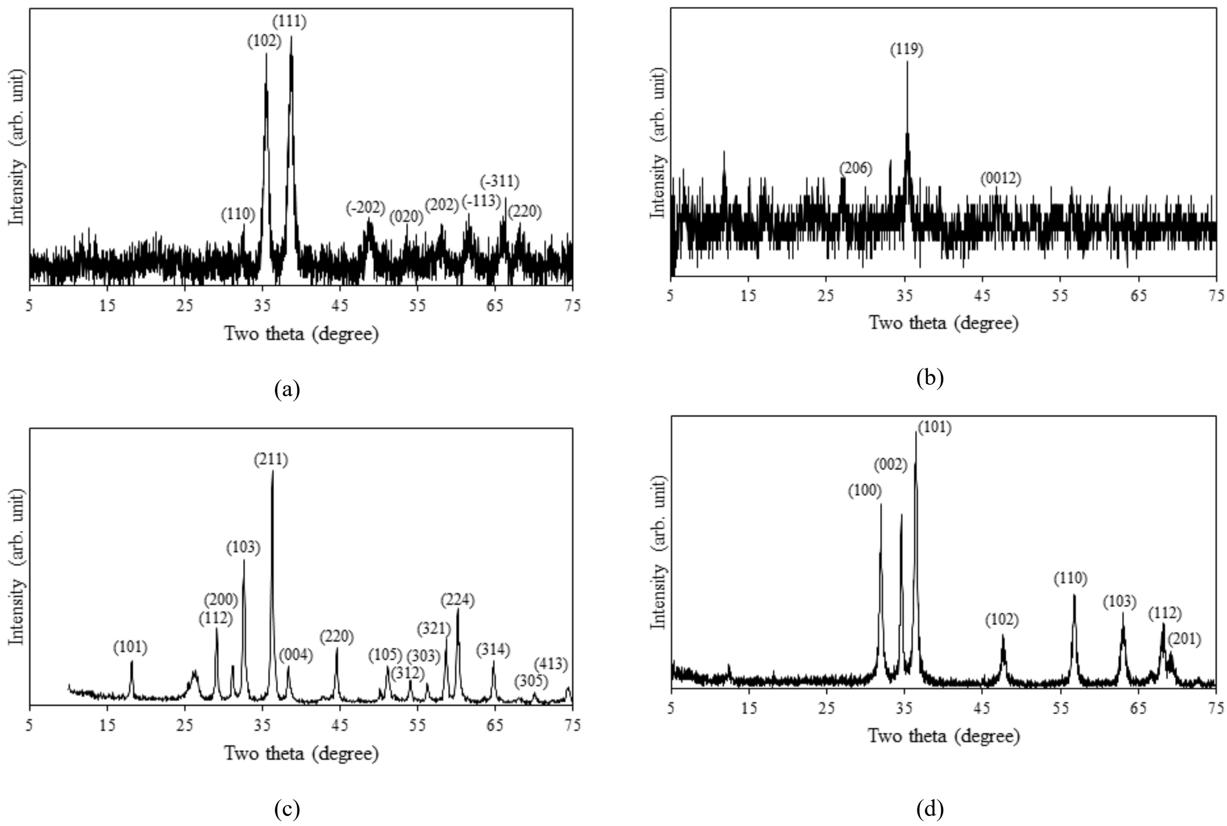

Fig. 2. XRD patterns of GO platelets which covered with a) CuO, b) Fe_2O_3, c) Mn_3O_4 and d) ZnO

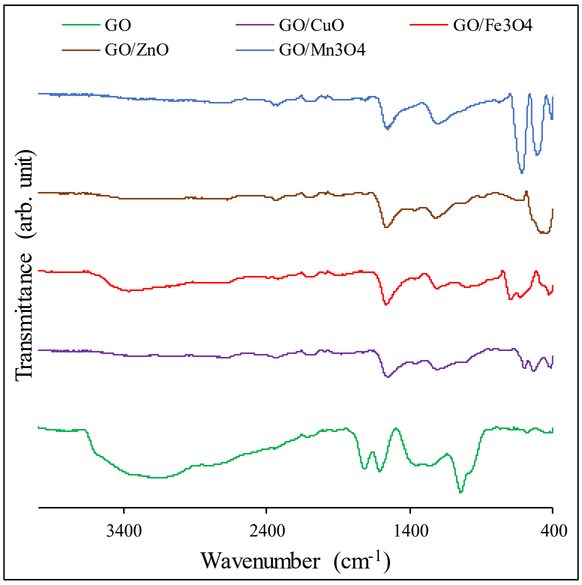

Fig. 3. FTIR Spectra of Metal oxide-GO platelets

the success of GO reduction process during the synthesis of composite powders.

SEM micrographs and corresponding EDS spectra GO platelets covered with CuO, Fe_2O_3, Mn_3O_4 and ZnO are shown in figure 4a to d, respectively. As illustrated, all samples were composed mainly of nano particles which were irregularly precipitated on the surface of GO platelets. As expected, very fine particles in nano range dimension were agglomerated in some locations. Moreover, all EDS spectra confirm the formation of corresponding metal oxides (MO).

UV- Visible spectra of samples are shown in figure 5. To estimate the optical band gap value, the Tauc method was used. This method assumes that the energy-dependent absorption coefficient α can be written by the following equation:

$$(\alpha h\nu)^{1/n} = B(h\nu - E_g) \quad (1)$$

where, h, ν, E_g and B are the Planck constant, the photon's frequency, the band gap energy, and a constant, respectively [20]. In practice, the curve of $(\alpha h\nu)^n$ versus hν should be drawn, where n =2 and 0.5 for direct and indirect transitions, respectively. Since all metal oxides and GO has direct transition, band gap values of samples were estimated based on the spectra and Tauc equation by plotting $(\alpha h\nu)^2$ versus hν (figure 6), and listed in Table 1. As illustrated, band gap values of nanocomposite powders were less than that of GO platelets. For comparison, some data of researchers added to the Table 1. It should be noted that band gap value of GO nanoplatelets depends on the different size and other characteristics. As mentioned before, various mechanisms are responsible for this phenomenon [12, 16–18].

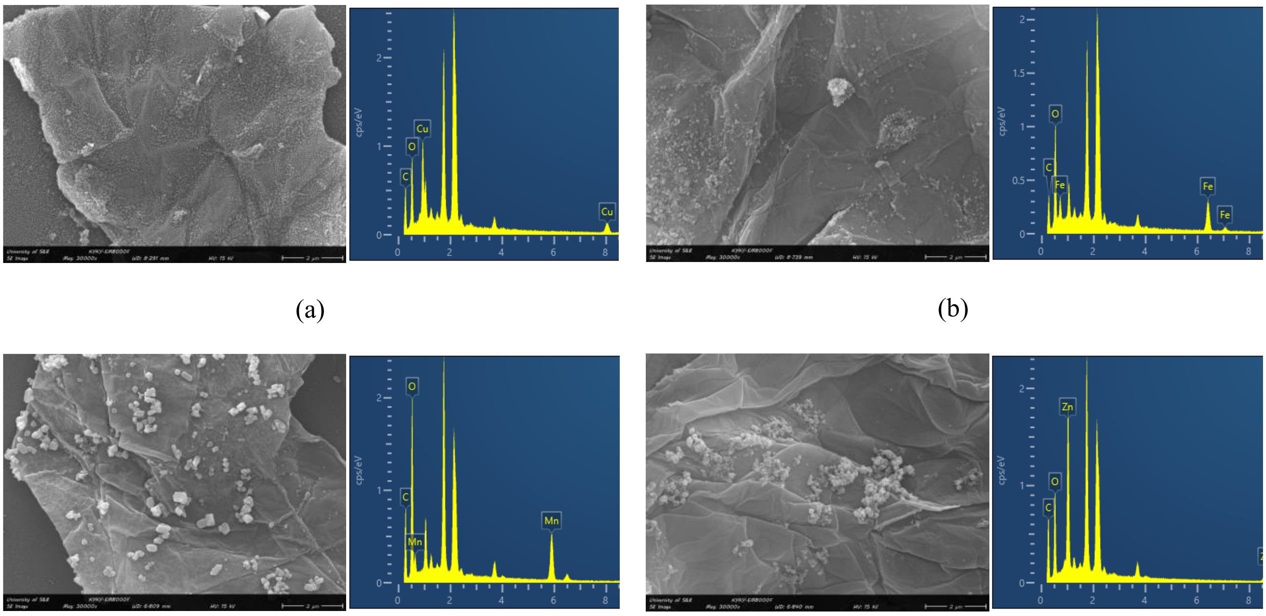

Fig. 4. SEM micrographs and corresponding EDS spectra of GO platelets which covered with a) CuO, b) Fe_2O_3, c) Mn_3O_4 and d) ZnO

In metal oxide/graphene oxide (MO/GO) nanocomposites, the observed band gap reduction of GO is generally attributed to interfacial electronic interactions and chemical modifications. The deposition of metal oxide nanoparticles onto GO sheets can induce Schottky-type heterojunction formation and interfacial charge transfer, leading to a shift in the Fermi level and the emergence of new electronic states at the interface. Concurrently, synthesis processes, particularly hydrothermal or thermal treatments, may partially remove oxygen-containing

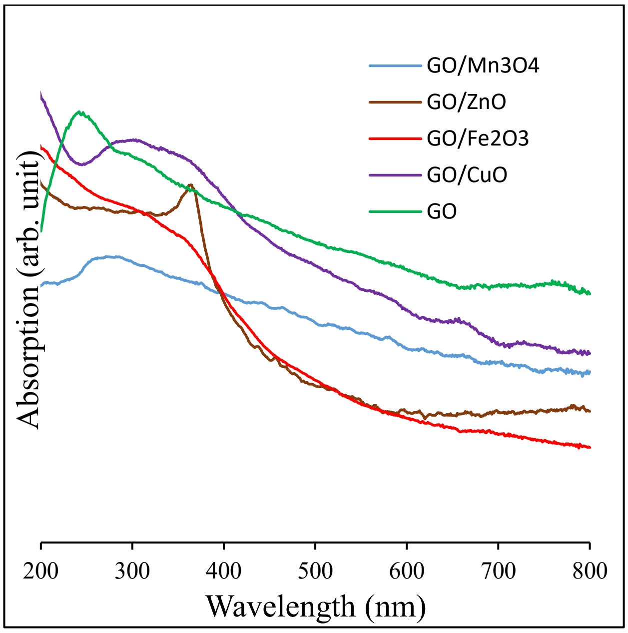

Fig. 5. UV- Visible spectra of Metal oxide-GO platelets

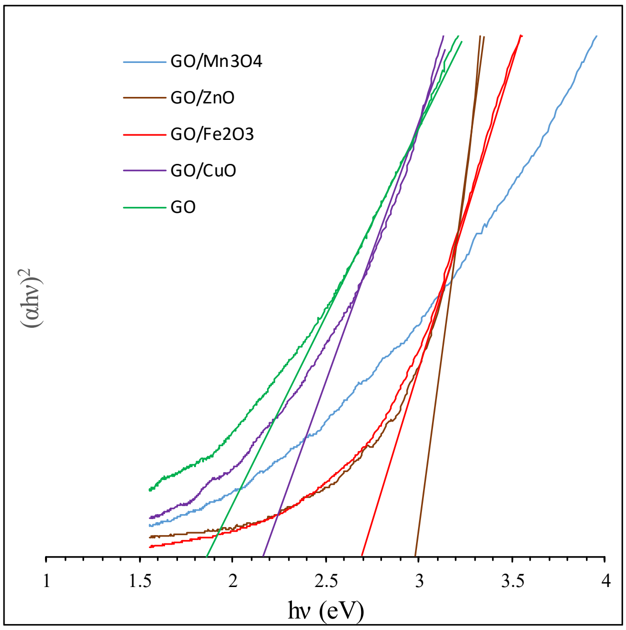

Fig. 6. $(\alpha h\nu)^2$ versus hν of Metal oxide-GO platelets

functional groups from GO, restoring sp^2 domains and improving π-conjugation, which introduces mid-gap states and facilitates electronic transitions. In addition, coordination between metal ions and oxygen functionalities on GO can act as chemical doping, generating impurity levels and defect-related states within the band structure. The combined effect of interfacial charge redistribution, partial structural restoration, and dopant-induced electronic states ultimately contributes to the narrowing of the band gap in these nanocomposite systems.

Table 1
Band gaps of GO and GO/MO composite powders.

Composition		GO	GO/CuO	GO/Fe_2O_3	GO/ZnO	GO/Mn_3O_4
Band gap (eV)	Present work	3.28	2.36	2.6	3.08	2.52
	Prabhu et.al. [26]	3.13	–	–	3.03	–
	Mubeen et.al. [27]	3.36	2.14	–	–	–
	Zainab et.al [28]	3.93	–	2.2	–	–

CONCLUSIONS

The present work focused on the precipitation synthesis of metal oxide nanoparticles on the Graphene oxide platelets. XRD patterns showed that nano-crystalline Metal oxide phases with no minor phase were obtained. FTIR spectra confirmed the presence of characteristic bands of Cu–O/Fe–O/Zn–O/Mn–O bonds in the samples. SEM Micrographs revealed that all samples consisted of nanoparticles which were synthesized on the surface of Graphene oxide platelets. Furthermore, the notable decrease of the GO-MO band gap values in comparison with GO further supports the creation of new energy bands and also formation of Interfacial charge transfer and Schottky junctions.

REFERENCES

[1] Khosravi H, Rastgou M, Tohidlou E. Enhancement of Interlaminar Shear Strength and Wear Resistance of E-Glass Fiber/Epoxy Composite With ZnO Nanoparticle-Anchored Graphene Oxide. Polym Adv Technol. 2025;36(9):e70359. doi:10.1002/pat.70359.

[2] Mahaki S, Khosravi H, Tohidlou E. Reinforcing effect of Fe2O3 nanoparticle-decorated graphene oxide on flexural and wear behaviors of epoxy composites. J Appl Polym Sci. 2022;139(48):e53228. doi:10.1002/app.53228.

[3] Mohseni F, Rezvani A, Khosravi H, Tohidlou E. On the Mechanical Properties of Copper Oxide (CuO)-Decorated Graphene Oxide/Epoxy Nanocomposites. Polym-Plast Technol Mater. 2025;64(2):158–169. doi:10.1080/25740881.2024.2393387.

[4] Ashokkumar SP, Vijeth H, Yesappa L, Niranjana M, Vandana M, Devendrappa H. Electrochemically synthesized polyaniline/copper oxide nano composites: To study optical band gap and electrochemical performance for energy storage devices. Inorg Chem Commun. 2020;115:107865. doi:10.1016/j.inoche.2020.107865.

[5] Choi J, Oh H, Han S-W, Ahn S, Noh J, Park JB. Preparation and characterization of graphene oxide supported Cu, Cu_2O, and CuO nanocomposites and their high photocatalytic activity for organic dye molecule. Curr Appl Phys. 2017;17(2):137–145. doi:10.1016/j.cap.2016.11.020.

[6] Gea S, et al. Facile synthesis of ZnO–Ag nanocomposite supported by graphene oxide with stabilised band-gap and wider visible-light region for photocatalyst application. J Mater Res Technol. 2022;19:2730–2741. doi:10.1016/j.jmrt.2022.05.184.

[7] Pei J, Zhao H, Yang F, Yan D. Graphene Oxide/Fe2O3 Nanocomposite as an Efficient Catalyst for Thermal Decomposition of Ammonium Perchlorate via the Vacuum-Freeze-Drying Method. Langmuir. 2021;37(20):6132–6138. doi:10.1021/acs.langmuir.1c00108.

[8] Goyat R, Saharan Y, Singh J, Umar A, Akbar S. Synthesis of Graphene-Based Nanocomposites for Environmental Remediation Applications: A Review. Molecules. 2022;27(19):6433. doi:10.3390/molecules27196433.

[9] Li M, et al. Preparation and antibacterial activity of graphene oxide/cuprous oxide/zinc oxide nanocomposite. Mater Res Express. 2021;8(12):125003. doi:10.1088/2053-1591/ac3950.

[10] Idisi DO, Aigbe UO, Ahia CC, Meyer EL. Graphene oxide: Fe_2O_3 nanocomposite: synthesis, properties, and applications. Carbon Lett. 2023;33(3):605–640. doi:10.1007/s42823-023-00469-4.

[11] Zhang W, et al. General synthesis of ultrafine metal oxide/reduced graphene oxide nanocomposites for ultrahigh-flux nanofiltration membrane. Nat Commun. 2022;13(1):471. doi:10.1038/s41467-022-28180-4.

[12] Avar B, Panigrahi M. Synthesis and Characterization of Binary Reduced Graphene Oxide/Metal Oxide Nanocomposites. Phys Chem Sol State. 2022;23(1):101–112. doi:10.15330/pcss.23.1.101-112.

[13] González-Moreno FI, Tolentino-Hernández RV, Espinosa-Faller FJ. Optical, structural and morphology study of Cu_2O/Cu and GO/Cu_2O/Cu films prepared by pulsed electrodeposition and electrophoresis. J Phys: Conf Ser. 2024;2699(1):012017. doi:10.1088/1742-6596/2699/1/012017.

[14] Di Bartolomeo A. Graphene Schottky diodes: An experimental review of the rectifying graphene/semiconductor heterojunction. Phys Rep. 2016;606:1–58. doi:10.1016/j.physrep.2015.10.003.

[15] Khairir NS, et al. Schottky behavior of reduced graphene oxide at various operating temperatures. Surf Interfaces. 2017;6:229–236. doi:10.1016/j.surfin.2016.10.004.

[16] Vuong Hoan NT, Anh Thu NT, van Duc H, Cuong ND, Quang Khieu D, Vo V. Fe3O4/Reduced Graphene Oxide Nanocomposite: Synthesis and Its Application for Toxic Metal Ion Removal. J Chem. 2016;2016(1):2418172. doi:10.1155/2016/2418172.

[17] Jamjoum HAA, Umar K, Adnan R, Razali MR, Mohamad Ibrahim MN. Synthesis, Characterization,

and Photocatalytic Activities of Graphene Oxide/metal Oxides Nanocomposites: A Review. Front Chem. 2021;9. Available from: https://www.frontiersin.org/journals/chemistry/articles/10.3389/fchem.2021.752276

[18] Nagarani S, Sasikala G, Satheesh K, Yuvaraj M, Jayavel R. Synthesis and characterization of binary transition metal oxide/reduced graphene oxide nanocomposites and its enhanced electrochemical properties for supercapacitor applications. J Mater Sci: Mater Electron. 2018;29(14):11738–11748. doi:10.1007/s10854-018-9272-0.

[19] Abbasian AR, Shafiee Afarani M. One-step solution combustion synthesis and characterization of ZnFe2O4 and ZnFe1.6O4 nanoparticles. Appl Phys A. 2019;125(10). doi:10.1007/s00339-019-3017-7.

[20] Makuła P, Pacia M, Macyk W. How to Correctly Determine the Band Gap Energy of Modified Semiconductor Photocatalysts Based on UV–Vis Spectra. J Phys Chem Lett. 2018;9(23):6814–6817. doi:10.1021/acs.jpclett.8b02892.

[21] Piri F, Shafiee Afarani M, Arabi AM. Synthesis of copper oxide quantum dots: effect of surface modifiers. Mater Res Express. 2019;6(12):125006. doi:10.1088/2053-1591/ab548d.

[22] Chu H-A, Sackett H, Babcock GT. Identification of a Mn−O−Mn Cluster Vibrational Mode of the Oxygen-Evolving Complex in Photosystem II by Low-Frequency FTIR Spectroscopy. Biochemistry. 2000;39(47):14371–14376. doi:10.1021/bi001751g.

[23] Dehdashti F, Shirkani H, Mehrabi M, Ahmadi A. Facile and green synthesis of α-Fe2O3 nanoparticles stabilized with chitosan for phototherapy with 808 nm laser irradiation. Sci Rep. 2025;15(1):32269. doi:10.1038/s41598-025-17797-2.

[24] Balogun SW, James OO, Sanusi YK, Olayinka OH. Green synthesis and characterization of zinc oxide nanoparticles using bashful (Mimosa pudica), leaf extract: a precursor for organic electronics applications. SN Appl Sci. 2020;2(3):504. doi:10.1007/s42452-020-2127-3.

[25] Zahiri M, Shafiee Afarani M, Arabi AM. Combustion Synthesis of ZnO/ZnS Nanocomposite Phosphors. J Fluoresc. 2019;29(5):1227–1239. doi:10.1007/s10895-019-02434-9.

[26] Prabhu S, et al. Synthesis, structural and optical properties of ZnO spindle/reduced graphene oxide composites with enhanced photocatalytic activity under visible light irradiation. Opt Mater. 2018;79:186–195. doi:10.1016/j.optmat.2018.02.061.

[27] Mubeen et al K. "Band structure tuning of ZnO/CuO composites for enhanced photocatalytic activity," Journal of Saudi Chemical Society,2023;27(3):101639, doi: 10.1016/j.jscs.2023.101639.

[28] Zainab S, Azeem M, Awan SU, Rizwan S, Iqbal N, and Rashid J. "Optimization of bandgap reduction in 2-dimensional GO nanosheets and nanocomposites of GO/iron-oxide for electronic device applications," Scientific Reports, 2023;13(1):6954 doi: 10.1038/s41598-023-33200-4.